arXiv:1903.12039v1 [astro-ph.GA] 28 Mar 2019

Masses of RR Lyrae Stars with Different Chemical Abundances in the Galactic Field

V. A. Marsakov, M. L. Gozha, V. V. Koval'
Southern Federal University, Rostov-on-Don, Russia
e-mail: marsakov@sfedu.ru, gozha_marina@mail.ru, vvkoval@sfedu.ru

accepted 2019, Astronomy Reports, Vol. 63, No. 3, pp. 203-211

Abstract

The surface gravities and effective temperatures have been added to a compilative catalog published earlier, which includes the relative abundances of several chemical elements for 100 field RR Lyrae stars. These atmoshperic parameters and evolutionary tracks from the Dartmouth database are used to determine the masses of the stars and perform a comparative analysis of the properties of RR Lyrae stars with different chemical compositions. The masses of metal-rich ([Fe/H] > -0.5) RR Lyrae stars with thin disk kinematics are in the range $(0.51 - 0.60)M_\odot$. Only stars with initial masses exceeding $1M_\odot$ can reach the horizontal branch during the life time of this subsystem. To become an RR Lyrae variable, a star must have lost approximately half of its mass during the red-giant phase. The appearance of such young, metal-rich RR Lyrae stars is possibly due to high initial helium abundances of their progenitors. According to the Dartmouth evolutionary tracks for Y = 0.4, a star with an initial mass as low as $0.8M_\odot$ could evolve to become an RR Lyrae variable during this time. Such stars should have lost $(0.2 - 0.3)M_\odot$ in the red-giant phase, which seems quite realistic. Populations of red giants and RR Lyrae stars with such high helium abundances have already been discovered in the bulge; some of these could easily be transported to the solar neighborhood as a consequence of perturbations due to inhomogeneities of the Galaxys gravitational potential.

Key words: RR Lyrae stars, chemical composition, kinematics, Galaxy (Milky Way).

1 Introduction

This paper continues our studies of RR Lyrae variables in the Galactic field initiated in [1, 2, 3]. These papers describe a catalog we have compiled containing the positions, velocities, and metal abundances of 415 field RR Lyrae stars, along with the relative abundances [el/Fe] of 12 elements for 100 RR Lyrae stars, including four α-process elements (Mg, Ca, Si, and Ti). We have used this catalog to study the relationships between the chemical properties of field RR Lyrae stars and their spatial and kinematic characteristics. In particular, we demonstrated that, despite the high ages usually claimed for these stars, the RR Lyrae population includes representatives of the youngest Galaxy subsystem, the thin disk. We also pointed out the problem of the existence of metal-rich RR Lyrae stars with [Fe/H] > -0.5. According to theoretical computations, the initial masses of these stars must have had in order for them to reach the horizontal branch are fairly low, $(0.55 - 0.8)M_\odot$ [4], and the evolution of such stars should take more than 10 billion years; i. e., more than the age of the thin-disk subsystem in the Galaxy. Higher-mass metal-rich stars evolve to the region of the red clump, outside the instability strip, and cannot become variables. However, the kinematics and chemical abundances of these stars derived in our study testify that they very likely belong to the thin disk and have younger ages. Some 70 years ago, Kukarkin [5] noted the presence of "peculiar" field RR Lyrae stars (called short-period Cepheids at that time) with periods below 0.43 days, which were not present in globular clusters and showed a stronger concentration to the Galactic plane than RR Lyrae

variables with longer periods. Later, most of these were found to be rich in metals. Despite the long history of their studies, the nature of metal-rich RR Lyrae stars remains incompletely understood. A semi-empirical explanation of the origin of metal-rich, comparatively young RR Lyrae stars suggested in [6] is that they result from the loss of a considerable fraction of a star's mass ($\sim 0.5 M_{\odot}$) during the red-giant evolution phase. This idea did not become popular, although it was also never disproved. The physical processes of metal-rich and metal-poor RR Lyrae stars were also found to differ. For example, the processes operating during the pulsations of these variables were studied in detail in [7], with considerable differences in the envelope kinematics found for metal-rich ([Fe/H] > -1.0) and metal-poor RR Lyrae stars. Chadid et al. [7] concluded that, although all RRab variables were horizontal-branch stars, metal-rich RR Lyrae stars had a different specific nature of their own.

It was suggested in [8] that the metal-richest and longest-period RR Lyrae variable in our list (KP Cyg) is most likely a classical Cepheid with an ultra-short period. It is possible that all or some metal-rich RR Lyrae stars could also be Cepheids pulsating in overtones with periods below one day. Such Cepheids have already been discovered in the Large and Small Magellanic Clouds through the OGLE project. Therefore, we suggested in [1, 3] that we should look for the origins of the kinematic and chemical youth of metal-rich RR Lyrae stars in their classification as variable stars. In this case, however, their masses should be even higher than for lower-temperature RR Lyrae stars, in contradiction with the general trend for the masses of horizontal-branch star to increase with decreasing temperature. Indeed, the effective temperatures and surface gravities were found in [7] to be higher for metal-rich RR Lyrae stars compared to metal-poor ones. At the same time, according to theoretical computations, the masses of horizontal-branch stars should increase with their surface gravity ($\log g$); however, on the contrary, their masses decrease with increasing metallicity. Thus, it is difficult to draw any conclusions about the mass of a particular RR Lyrae star *a priori*.

Taking all this into account, our study is aimed at determining the masses of field RR Lyrae stars with published elemental abundances and atmospheric parameters using theoretical evolutionary tracks, together with a comparative analysis of the properties of metal-rich RR Lyrae stars in order to improve our understanding of their nature.

2 INPUT DATA

We found the effective temperatures $T_{\rm eff}$ and surface gravities $\log g$ for all 100 RR Lyrae variables in our catalog in the same 25 publications from 1995–2017 that had earlier been our sources of information on the elemental abundances in the atmospheres of these stars [1]. References to these publications can be found in our online catalog.

The atmospheric parameters of periodically pulsating RR Lyrae variables depend on their pulsation phase. It is believed that the most accurate atmospheric parameters can be obtained during the phase of minimum brightness ($\phi \sim 0.8$), when the star's atmosphere is essentially not affected by pulsations (e.g., [9, 10]). The basic parameters of the stellar atmospheres, $T_{\rm eff}$ and $\log g$, can be determining using both spectroscopic and photometric methods. Some researchers have recommended preferred parameter values among those they have obtained using various methods. When recommendation is expressed by the authors of the studies used, we calculated the parameters averaged over phase and over values obtained using different methods. Taking into account only values for phases close to the minimum brightness did not lead to any significant change in the average values for $T_{\rm eff}$ and $\log g$.

Most researchers had estimated the uncertainties of the parameters they derived. Spectroscopic determinations of $T_{\rm eff}$ and $\log g$ have uncertainties from 40 to 300 K and from 0.1 to 0.5 dex, with the mean values being $\varepsilon(T_{\rm eff}) = 115$ K and $\varepsilon(\log g) = 0.24$. The uncertainties of photometrically determined values of $T_{\rm eff}$ and $\log g$ vary from 100 to 250 K and from 0.1 to 0.3 dex; the mean uncertainties quoted for this method are $\varepsilon(T_{\rm eff}) = 170$ K and $\varepsilon(\log g) = 0.18$. The modes of the uncertainties using any methods are about 200 K for the effective temperature and 0.3 dex for the surface gravity. If there was no information available about the uncertainties in measured parameters,

we adopted these uncertainties.

The effective temperatures and surface gravities for 40 RR Lyrae variables were determined in two or more studies. For these stars, we calculated the weighted mean parameters using weights that were inversely proportional to the quoted uncertainties. We used these same RR Lyrae stars to plot distributions of the deviations of both parameters from the corresponding weighted mean values for all the determinations. These distributions were successfully represented with Gaussian curves, indicating the random character of the differences between parameters obtained in different studies. The mean dispersions provide estimates of the external agreement of the parameters derived in different studies, $\varepsilon(T_{\rm eff}) = 226 \pm 15$ K and $\varepsilon(\log g) = 0.25 \pm 0.02$. We can see that this external agreement is comparable to the uncertainties averaged over all the methods.

Table 1 presents atmospheric parameters for the 100 RR Lyrae stars with known elemental abundances. The columns of this table contain (1) the name of the star; (2) the metallicities from [1]; (3) the relative abundances of α-process elements, [α/Fe] (see below); (4)–(6) data on the effective temperature: the value adopted in this paper (TP) and the highest and lowest $T_{\rm eff}$ values among those recommended in publications or averaged over phase and methods, when $T_{\rm eff}$ values were taken from two or more papers; (7)–(9) analogous parameters for the surface gravity $\log g$; and (10) mass of the star determined using evolutionary tracks (see below).

Figure 1a plots the surface gravity $\log g$ versus the effective temperature $\log T_{\rm eff}$ for the 100 RR Lyrae stars of our sample. The filled black circles show the metal-richest stars, filled gray circles those with metallicities $-0.5 >$ [Fe/H] > -1.0, and open triangles the lowest-metallicity stars. The temperature and surface gravity uncertainties described above result in uncertainties in the derived masses $\varepsilon(M/M_{\odot}) \approx 0.015$. Figure 1 shows that the positions of metal-rich RR Lyrae stars in this diagram somewhat contradicts the conclusion of [7] that metal-rich RR Lyrae stars mainly have higher values of $\log g$ and of $\log T_{\rm eff}$ than do metal-poorer stars: in contrast to [7], our sample contains an appreciable number of low-metallicity RR Lyrae stars with higher temperatures than those of metal-rich stars. However, most of the low-metallicity RR Lyrae stars that form a clump in the diagram are cooler. Note that all the metal-poor RR Lyrae stars in the clump (with the exception of HH Pup) belong to the halo or thick disk according to their kinematics; i. e., they have a high ages that would enable initially low-mass stars to reach the horizontal branch.

We used the spatial and kinematic data of Dambis et al. [11] in our sample of RR Lyrae stars [1], where the magnitude in the K_S infrared filter was applied to introduce interstellar reddening corrections and to calibrate the distances to the RR Lyrae stars. We emphasize that RR Lyrae variables remain one of the few kinds of objects that are easy to identify at considerable distances, where direct parallax measurements are not possible, even using modern instruments. It is thus interesting to check how the absolute magnitudes derived from the calibration agree with the theoretical values. After replacing the metallicities in the formula from [11] with our spectroscopic data, we calculated the relationship between the absolute magnitudes and the variability periods of RR Lyrae stars from the same catalog: $M_{Ks} = -0.769 + 0.088 \cdot [{\rm Fe/H}]_{\rm Sp} - 2.33 \cdot \log {\rm P_F}$, where $[{\rm Fe/H}]_{\rm Sp}$ are the spectroscopic metallicities and P_F are the fundamental pulsation periods of the RR Lyrae stars.

Figure 1b plots the absolute magnitude M_{Ks} versus the effective temperature for the same stars. To facilitate a comparison of these two diagrams, we plotted evolutionary tracks for stars of various masses with the same input parameters on both diagrams. In general, the stars with different metallicities have approximately similar distributions, but the surface gravities and calculated absolute magnitudes for some stars contradict each other. In particular, SDSS J1707+58 and KP Cyg have high $\log g$ values, but high luminosities. On the contrary, HH Pup has a fairly low $\log g$ value, but its luminosity is also low. We will not consider the origins of such discrepancies for each RR Lyrae star, as this requires a special investigation. The stars displaying the strongest deviations are marked in the diagrams. Note that we were able to find only upper or lower limits to the masses of FV Aqr, DO Vir, and CM Leo, and it was not possible to determine the masses of CU Com and SDSS J1707+58 because their $\log g$ values were outside the range specified by the limits of the grid of models used for horizontal-branch stars.

Let us note some general patterns shown by Fig. 1. It is striking that stars in the $\log T_{\rm eff}$ – M_{Ks} diagram are aligned almost parallel to the horizontal axis, while they lie parallel to the theoretical lines for constant masses in the $\log T_{\rm eff}$ – $\log g$ diagram. Two of the highest-metallicity RR Lyrae stars (KP Cyg and UY CrB) are the brightest in the $\log T_{eff}$ – M_{Ks} diagram, although the other metal-rich RR Lyrae stars have the lowest luminosities. Lower-metallicity RR Lyrae stars ($-1.0 <$ [Fe/H] < -0.5) also lie near the lower boundary of the diagram, while they are considerably higher than the metal-richest stars in the $\log T_{\rm eff}$ – $\log g$ diagram, and low-metallicty RR Lyrae stars are only slightly brighter. Apparently the atmospheric parameters determined spectroscopically are more correct than the distances and absolute magnitudes derived from calibration relations. In addition, these parameters are also computed more reliably using model atmospheres. Thus, we prefer to determine the masses using these parameters.

3 MASSES OF THE RR LYRAE STARS

We determined the masses of the RR Lyrae stars in our sample using evolutionary tracks from the Dartmouth database [12]. These theoretical computations can be used to take into account not only the general abundances of heavy elements [Fe/H] in the stars, but also the relative abundances of α-process elements [α/Fe], with the helium abundance Y being proportional to the metallicity. There is also the possibility of specifying the enhanced helium abundances. The evolutionary tracks for discrete masses were given in [Fe/H] increments of 0.5 dex and [α/Fe] increments of 0.2 dex. We found the mass of each RR Lyrae star by interpolating between all these parameters. To determine [α/Fe], we averaged the relative abundances of magnesium, calcium, silicon, and titanium given in [1]. The abundances of all these four elements are known for most stars in our sample. If there was no information on one of the elements listed above, we found the average for the other known α-process elements (the corresponding [α/Fe] values are presented in Table 1). There is only one star in our catalog with no abundances of α-process elements (UY CrB). In order to find the mass of this variable, we used the abundance [α/Fe] = 0.0 typical of solar-metallicity stars, similar to the metallicity of UY CrB (Increasing [α/Fe] does not significantly change the mass of this star derived from the tracks.). The resulting masses of the RR Lyrae stars are collected in the last column of Table 1.

As an example, Fig. 1a shows two evolutionary tracks of different masses for the solar chemical composition and two tracks for a metallicity a factor of 100 lower, with typically increased relative abundances of α-process elements ([α/Fe] = 0.4), which are approximate upper and lower limits for the RR Lyrae stars in our sample in the diagram. The evolutionary tracks for lower masses and any metallicity appear in the upper part of the diagram, as a rule, at higher temperatures, while tracks for high masses do not reach the instability strip in the lower part of the diagram, and are completely outside its low-temperature boundary. As a result, horizontal-branch stars with the same atmospheric parameters will have higher masses for lower metallicities. A decrease in the relative α-process element abundances also results in a slight shift towards higher masses. We can see from the $\log T_{\rm eff}$ – $\log g$ diagram that the range of basic atmospheric parameters and the range of masses are much narrower for high-metallicity RR Lyrae stars, and the masses are, on average, lower than for low-metallicity RR Lyrae stars.

Continuing our comparison with the absolute magnitudes obtained via calibration, we plotted the same evolutionary tracks in Fig. 1b. The $\log T_{\rm eff}$ – M_{Ks} diagram shows that, if the absolute magnitudes M_{Ks} are used, the range of derived masses for our RR Lyrae stars shifts considerably towards higher masses, leaving the upper part of the low-mass region of the diagram unoccupied, and slightly displacing the lower boundary downwards. As a result, the lowest RR Lyrae stars in this diagram lie in the region that is not reached by the high-mass evolutionary tracks from the theoretical computations we used. That is, the absolute magnitudes of the RR Lyrae stars found from their variation periods and metallicities disagree with the theoretical positions for horizontal-branch stars, making it impossible to determine masses for many of them from these data. The

calibration of [11] apparently requires some correction.

Figure 2 shows the dependences of the derived masses of the RR Lyrae stars on their atmospheric parameters and chemical compositions. Different symbols are used for stars belonging to different subsystems of the Galaxy. We distinguished the subsystems by applying the kinematic criterion from [13], where the components of the space velocities are used to calculate probabilities for an RR Lyrae star to belong to the thin disk, thick disk, or halo subsystems (for more details, see [1]). It was assumed here that the the components of the stellar space velocities in each of the subsystems have normal distributions.

Figure 2a displays the dependence of the mass on the metallicity. The lower mass limit remains the same for any metallicity, while the upper mass limit grows linearly over the entire range of metallicities. In the range [Fe/H] > -1.0, however, we observe a jump-like stronger concentration of stars toward the lower mass limit than in the lower-metallicity range. This behavior is completely unrelated to whether the stars' kinematics ascribe them to a particular subsystem, i. e., to their space velocities, but is related to their metallicities: all metal-rich RR Lyrae stars in the thick disk and halo have low masses. Note that the transition through the boundary value, [Fe/H] $= -1.0$, also results in an abrupt increase in the scatter of the distances from the Galactic plane, as well as an increase in the dispersion of the space velocities for our RR Lyrae stars (see [[1], Fig. 1]). This behavior of the velocity dispersion motivated the traditional subdivision of RR Lyrae stars at this metallicity into those belonging to the thick disk and halo, despite the fact that it is precisely the kinematics that defines the spatial distribution of the stars in the subsystems. Nevertheless, we suggest that the jump in the masses correlates with the jump in the velocities, simply because both parameters are related through the metallicity, although, physically speaking, the mass does not depend on the velocity. Note that globular clusters also exhibit abrupt changes in their spatial and kinematic properties when the same metallicity is crossed (e.g., [14]).

The expected exponential relations are found for each subsystem's RR Lyrae stars in the $\log g$ – $M/M_{\odot}$ diagram, Fig. 2b. The sequences of thin-disk and halo RR Lyrae stars essentially do not meet; as we can see from the [Fe/H] – $M/M_{\odot}$ diagram, the metallicities of the stars in these subsystems do not overlap. In addition, the masses of metal-rich RR Lyrae stars are always less than those of metal-poor ones for a given $\log g$. On the other hand, the thick-disk strip partially covers the sequences of both subsystems, due to its very wide metallicity range. Further, the $\log T_{\rm eff}$ – $M/M_{\odot}$ diagram in Fig. 2c shows the masses of RR Lyrae stars in different subsystems at different temperatures. Here, we note that, independent of the kinematic membership in a particular subsystem, the upper mass limit for the RR Lyrae stars increases with decreasing temperature, while the lower limit is independent of temperature. The last diagram, [α/Fe] – $M/M_{\odot}$ in Fig. 2d, also displays a mass increase with increasing relative abundance of α- process elements. Since there are no RR Lyrae stars with [α/Fe] ~ 0.15, this suggests the presence of an abrupt increase in the mean mass when this boundary is crossed. This results from the fact that the relative abundances of α-process element for most thin-disk RR Lyrae stars are nearly solar, but they abruptly increase for metal-poorer stars.

4 DISCUSSION

Our study shows that virtually all effective temperatures ($T_{\rm eff}$) and surface gravities ($\log g$) for field RR Lyrae variables in the literature enter the instability strip for corresponding theoretical evolutionary tracks of horizontal-branch stars, enabling derivation of the stellar masses. We suggest that this is reflects the correctness of their derived atmospheric parameters. On the other hand, there is no such agreement for the absolute magnitudes M_{Ks} derived for these stars from calibration relations for variability periods and metallicities. As a result, a large region in the theoretically identified area of variable stars in the $\log T_{\rm eff}$ – M_{Ks} diagram remains unoccupied, and a considerable fraction of our RR Lyrae stars lie in a region that they should not be able to enter according to the theoretical computations.

Our checks show that the values of M_{Ks} and $\log g$ are completely uncorrelated. This indicates

that the calibration of the absolute magnitudes of the RR Lyrae stars from their variability periods and metallicities is not quite correct. Therefore, we derived the masses solely based on atmospheric parameters determined using spectra. As a result, we found that the lower mass limits for metal-rich and metal-poor RR Lyrae stars coincide, and are approximately half a solar mass. At the same time, the upper mass limit decreases rapidly with increasing metallicity. The low-metallicity, low-mass RR Lyrae stars mainly belong to the halo subsystem, or less frequently to the thick disk, indicating that they are very old stars and pose no problem. However, in the traditional assumption that a stars mass loss in the red-giant phase and the subsequent helium flash is of order $(0.1-0.2)M_{\odot}$ (see [6] and references therein), so find that the initial masses for most of the metal-rich stars are theoretically too low for them to reach the horizontal branch during a time interval shorter than the age of the thin disk subsystem.

An analysis of the elemental abundances in nearby stars demonstrates that the thick disk also contains old stars with the solar metallicity and low relative abundances of α-process elements, but with ages exceeding 10 billion years (e.g., [15]). However, the RR Lyrae stars with solar abundances also exhibit very "young" kinematics, typical of the thin disk rather than this subsystem. If we suppose that these are higher-mass stars — Cepheids pulsating in an overtone, i. e., with a shorter than usual period — they should also display systematically lower surface gravities and temperatures characteristic of Cepheids, but this is not observed.

There is another possible origin for these stars. It was found for nearby stars displaying thin-disk kinematics that a small number of stars with solar abundances already appeared in the thin disk during the very first stages of its formation (see [[16], Fig. 8]). They are the so-called old metal-rich stars; it is believed that they were born near the Galactic center and then migrated from there due to perturbations from asymmetric gravitational components, such as a central bar or spiral density waves [17]. According to the Dartmouth evolutionary tracks, a star with an initial mass of $1.05M_{\odot}$ and solar elemental abundances should reach the horizontal branch in $\sim$ 10 billion years, which is usually believed to be the age of the thin disk. However, in order to enter the instability strip at the horizontal branch, stars with such high masses must lose about half their mass during the red-giant phase, as was suggested in [6].

We can further reduce the initial mass if the initial helium abundances in the progenitors of metal-rich RR Lyrae stars were higher. According to the Dartmouth theoretical computations, even a star with a mass of $0.8M_{\odot}$ and an initial helium abundance of Y = 0.4 will reach the horizontal branch in $\sim$ 9.3 billion years. In order to enter the instability strip, such stars must lose $(0.2-0.3)M_{\odot}$ during the red-giant phase and the helium flash, but this is a quite realistic mass loss. In fact, modern computations of stellar models [18] demonstrate that stars with this initial mass can lose even more than $0.2M_{\odot}$ via their stellar winds by the end of their evolution on the red-giant branch, i. e., before the mass loss after the helium flash. However, we must assume the highest mass-loss rate in the empirical formula describing this process in this case. Furthermore, these same computations demonstrate that, with increasing helium abundance, such stars arrive at the higher-temperature part of the horizontal branch, like our metal-rich RR Lyrae stars in Fig. 1. Stars with enhanced helium abundances have already been detected in the bulge. For example, the recent paper [19] presents helium-abundance estimates for the population of RRab stars in the huge sample of RR Lyrae stars from the OGLE IV survey [20], obtained based on the fact that, according to the non-linear convective pulsation model, the shortest period of the fundamental RRab mode depends strongly on the helium abundance in the star. In particular, it is concluded in [19] that their results cannot exclude the presence of a small fraction of RRab stars with enhanced helium abundances in the bulge, similar to the abundances measured for bulge red-clump stars, with mean Y = 0.28-0.35 [21]. Studies of the helium abundances of field RR Lyrae variables that are currently in the solar neighborhood would provide useful information for verifying this conclusion.

ACKNOWLEDGMENTS

The authors are grateful to the anonymous referee for comments that have enabled us to improve the paper. This work has been supported by the Ministry of Education and Science of the Russian Federation (state contracts 3.5602.2017/BCh and 3.858.2017/4.6).

REFERENCES

[1] V. A. Marsakov, M. L. Gozha and V. V. Koval', Astron. Rep. **62**, 50 (2018).

[2] M. L. Gozha, V. A. Marsakov, and V. V. Koval', Astrophysics **61**, 41 (2018).

[3] V. A. Marsakov, M. L. Gozha, V. V. Koval', and E. I. Vorobyov, Astrophysics. **61**, 171 (2018).

[4] M. Marconi, G. Coppola, G. Bono, V. Braga, et al., Astrophys. J. **808**, 50 (2015).

[5] B. V. Kukarkin, Study of the Structure and Development of Stellar Systems Based on Studies of Variable Stars (Gos. Izdat. Tekh.-Teor. Liter., Moscow, Leningrad, 1949) [in Russian].

[6] R. E. Taam, R. P. Kraft, and N. Suntzeff, Astrophys. J. **207**, 201 (1976).

[7] M. Chadid, C. Sneden, and G. W. Preston, Astrophys. J. **835**, 187 (2017).

[8] S. M. Andrievsky, V. V. Kovtyukh, G. Wallerstein, S. A. Korotin, and W. Huang, Publ. Astron. Soc. Pacific. **122**, 877 (2010).

[9] D.L. Lambert, J.E. Heath, M. Lemke, and J. Drake, Astrophys. J. Suppl. Ser. **103**, 183 (1996).

[10] S. Liu, G. Zhao, Y.-Q. Chen, Y. Takeda, and S. Honda, Research in Astron. Astrophys. **13**, 1307 (2013).

[11] A. K. Dambis, L. N. Berdnikov, A. Y. Kniazev, et al., Monthly Not. R. Astron. Soc. **435**, 3206 (2013).

[12] A. Dotter, B. Chaboyer, D. Jevremovic, V. Kostov, E. Baron, and J.W. Fergusonet, Astrophys. J. Suppl. Ser. **178**, 89 (2008) http://stellar.dartmouth.edu/models/index.html

[13] T. Bensby, S. Feldzing, and I. Lungstrem, Astron. and Astrophys. **410**, 527 (2003).

[14] T. V. Borkova and V. A. Marsakov, Astron. Rep. **44**, 665 (2000).

[15] V. A. Marsakov and T. V. Borkova, Astron. Lett. **31**, 515 (2005).

[16] V. A. Marsakov and T. V. Borkova, Astron. Lett. **32**, 545 (2006).

[17] R. Schonrich, and J. Binney, Monthly Not. R. Astron. Soc. **396**, 203 (2009).

[18] X. Fu, A. Bressan, P. Marigo, L. Girardi, et al., Monthly Not. R. Astron. Soc. **476**, 496 (2018).

[19] M. Marconi, and D. Minniti, Astrophys. J. **853**, 20 (2018).

[20] P. Pietrukowicz, S. Kozowski, J. Skowron, I. Soszynski, et al., Astrophys. J. **811**, 113 (2015).

[21] Y.-W. Lee, and S. Jang, Astrophys. J. **833**, 236 (2016).

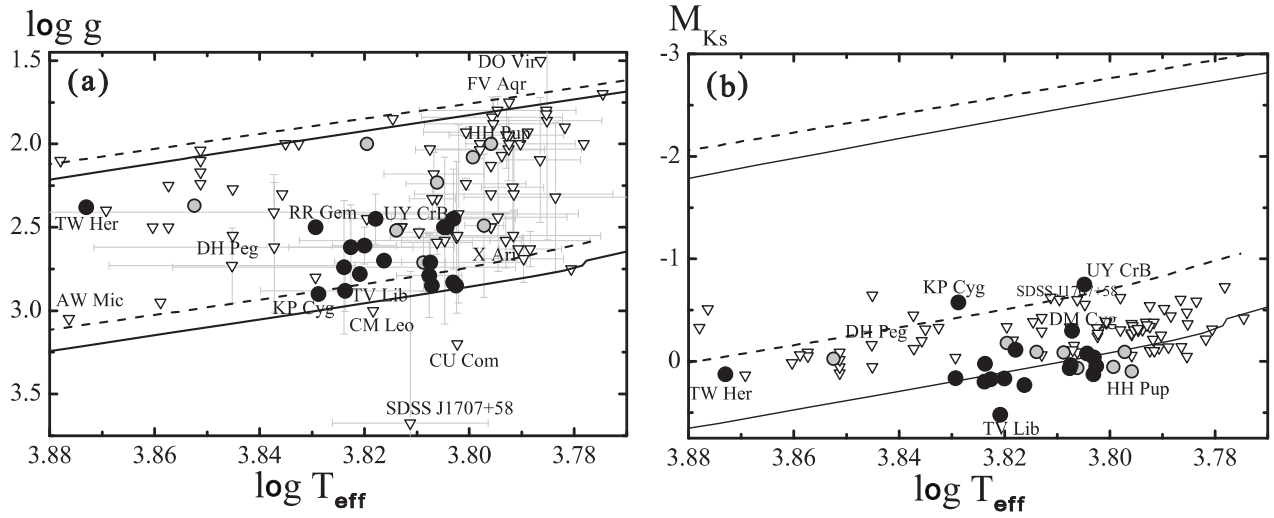


Figure 1: Relations between the effective temperature, $\log T_{eff}$, and (a) surface gravity, $\log g$, and (b) absolute magnitude, M_{Ks}, for the RR Lyrae stars in our sample. Black circles denote stars with [Fe/H] > -0.5, gray circles those with $-0.5 >$ [Fe/H] > -1.0, and open triangles the lowest-metallicity stars with [Fe/H] < -1.0. For RR Lyrae stars with atmospheric parameters determined in multiple studies, the bars mark the highest and lowest derived parameters for that RR Lyrae star. In both panels, two evolutionary tracks are plotted, for stars with the solar chemical composition and masses of 0.49 and 0.54 $M_{\odot}$ (upper and lower solid curves, respectively). The dashed curves show evolutionary tracks for stars with masses of 0.52 and $0.75 M_{\odot}$, metallicities a factor of hundred lower than the solar value, and relative abundances of α-process elements [α/Fe] $= 0.4$. The names of RR Lyrae stars that strongly deviate from the highest-density concentration of data points in various diagrams (including those in [1–3]) are marked.

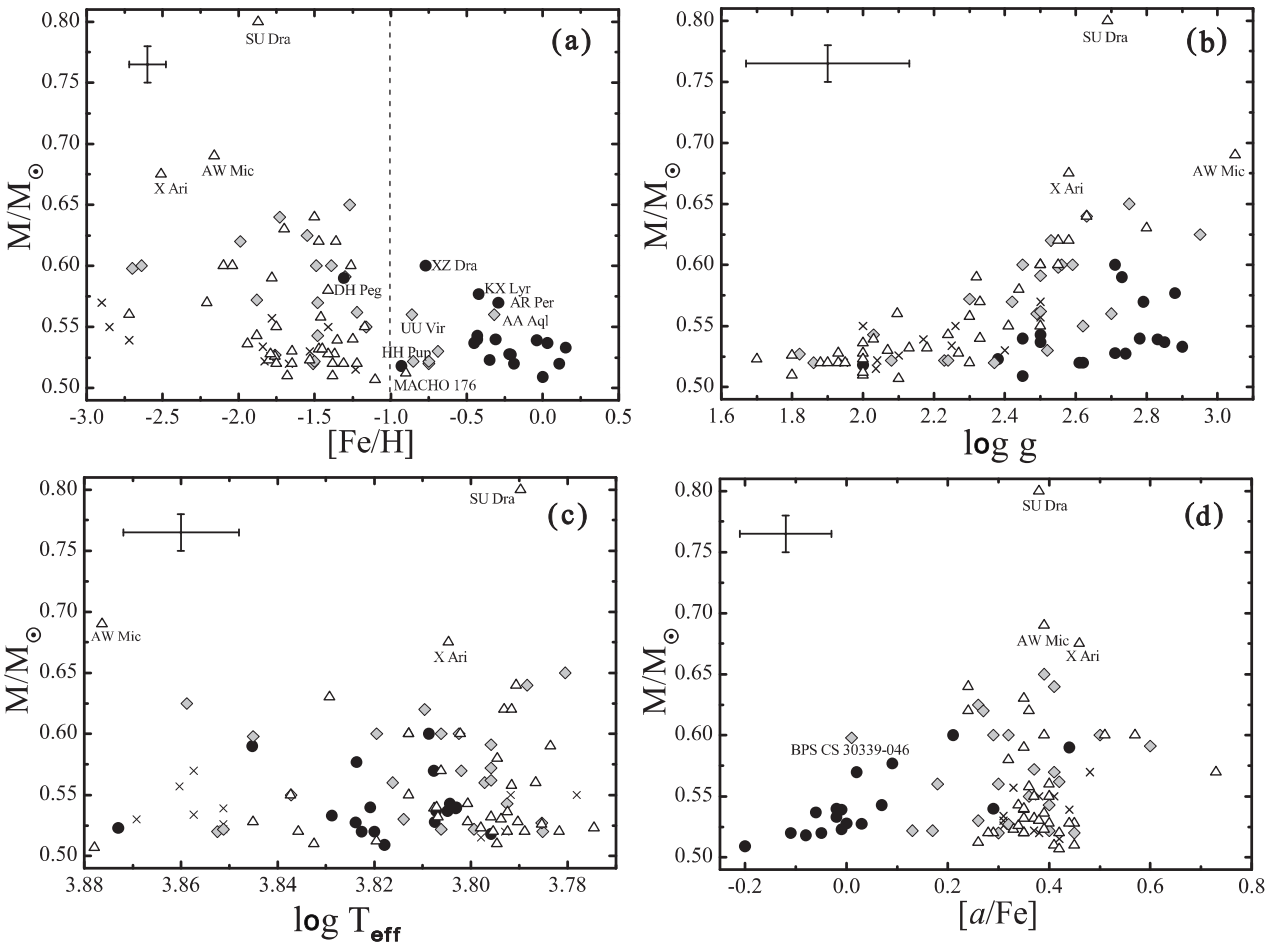


Figure 2: Masses of RR Lyrae stars in our sample versus (a) metallicity, (b) surface gravity, (c) effective temperature, and (d) relative abundances of α-process elements. The black circles show RR Lyrae stars belonging to the thin disk, according to their kinematics, gray diamonds those belonging to the thick disk, open triangles those belonging to the halo, and crosses RR Lyrae stars with no specific classification. The vertical dashed line is at [Fe/H] $= -1.0$.

Table 1: Astrophysical parameters of RR Lyrae stars

Star	Abundance, dex		$T_{\rm eff}$, K			$\log g$, dex			Mass, $M_\odot$
	[Fe/H]	[α/Fe]	TP	min	max	TP	min	max	
1	2	3	4	5	6	7	8	9	10
SW And	-0.22	0.00	6419	6184	6735	2.71	2.50	2.85	0.53
CI And	-0.43	0.07	6373			2.50			0.54
DR And	-1.37	0.40	6170	6000	6300	2.00			0.53
WY Ant	-1.88	0.34	6319	6150	6487	2.24	2.20	2.27	0.54
XZ Aps	-1.79	0.45	6319	6200	6438	1.93	1.90	1.95	0.53
BS Aps	-1.48	0.40	6202	6000	6404	2.03	1.80	2.18	0.54
AA Aql	-0.32	0.18	6550			2.70			0.56
SW Aqr	-1.38	0.28	6200			1.95			0.52
BR Aqr	-0.69	0.26	6515			2.52			0.53
DN Aqr	-1.76	0.34	6100			1.80			0.53
FV Aqr	-2.59	0.41	6200			1.75			< 0.54
X Ari	-2.51	0.46	6378	6109	6950	2.58	2.10	3.10	0.68
ASAS J085254-0300.3	-1.53	0.31	7400			2.40			0.53
ASAS J162158+0244.5	-1.84	0.31	7200			2.25			0.53
RS Boo	-0.21	0.03	6666	6233	7275	2.74	2.40	3.20	0.53
ST Boo	-1.73	0.41	6143	6081	6250	2.63	2.50	2.71	0.64
TW Boo	-1.47	0.37	6250			2.13			0.53
BPS CS 22881-039	-2.72	0.40	6117	5950	6170	2.10	1.85	2.60	0.56
BPS CS 22940-070	-1.41	0.38	6191	6130	6300	2.26	1.85	2.40	0.55
BPS CS 30317-056	-2.85	0.41	6000			2.00			0.55
BPS CS 30339-046	-2.70	0.01	7000			2.55			0.60
W CVn	-1.22	0.42	6250			2.50			0.56
UZ CVn	-2.21	0.73	6400			2.33			0.57
YZ Cap	-1.50	0.40	7100			2.24			0.52
RZ Cep	-2.10	0.57	6500			2.50			0.60
RR Cet	-1.48	0.41	6339	5966	6650	2.42	1.70	2.77	0.57
RX Cet	-1.38	0.45	6800			2.00			0.51
UU Cet	-1.36	0.36	6210	6165	6250	2.58	2.38	2.71	0.62
U Com	-1.41	0.44	7000			2.27			0.53
CU Com	-2.38	0.38	6343			3.20			-
UY CrB	-0.45		6380			2.50			0.54
W Crt	-0.75	0.17	6400			2.23			0.52
XZ Cyg	-1.50	0.24	6175			2.63			0.64
DM Cyg	0.03	-0.06	6415			2.85			0.54
KP Cyg	0.15	-0.02	6742			2.90			0.53
DX Del	-0.31	-0.02	6354	6150	6500	2.45	2.13	2.73	0.54
SU Dra	-1.87	0.38	6161	6083	6300	2.69	2.50	2.78	0.80
SW Dra	-1.27	0.39	6033			2.75			0.65
XZ Dra	-0.77	0.21	6438	6375	6500	2.71	2.50	2.85	0.60
AE Dra	-1.46	0.51	6525			1.85			0.51
SV Eri	-1.99	0.27	6450	6400	6500	2.53	2.50	2.55	0.62
BK Eri	-1.72	0.36	6840			2.00			0.51
CS Eri	-1.70	0.35	6750			2.80			0.63

1	2	3	4	5	6	7	8	9	10
SX For	-1.80	0.33	5950			1.70			0.52
RR Gem	0.01	-0.20	6750			2.50			0.51
SZ Gem	-1.65	0.42	6050			1.90			0.52
TY Gru	-1.88	0.37	6250			2.30			0.57
BO Gru	-1.83	0.37	7100			2.04			0.52
TW Her	-0.35	-0.01	7465			2.38			0.52
VX Her	-1.46	0.36	6188	5975	6525	2.30	2.05	2.72	0.56
VZ Her	-1.30	0.60	6250			2.50			0.59
DH Hya	-1.53	0.39	6280			2.00			0.52
DT Hya	-1.23	0.42	6280	6100	6460	2.04	2.00	2.10	0.52
V Ind	-1.45	0.35	6409	6267	6550	2.18	2.03	2.29	0.53
RR Leo	-1.39	0.50	6400	6300	6500	2.59	2.50	2.65	0.60
SS Leo	-1.75	0.37	6875	6100	7650	2.41	2.05	2.50	0.55
ST Leo	-1.31	0.29	6150			1.93			0.52
CM Leo	-1.93	0.42	6582			3.00			> 1.5
TV Lib	-0.43	0.29	6620			2.78			0.54
TT Lyn	-1.47	0.24	6189	6016	6500	2.55	2.45	2.75	0.62
RR Lyr	-1.49	0.29	6345	6125	6500	2.56	2.13	3.04	0.60
CN Lyr	-0.04	-0.01	6355			2.83			0.54
IO Lyr	-1.35	0.35	6420			2.03			0.54
KX Lyr	-0.42	0.09	6663	6495	7000	2.88	2.75	3.00	0.58
MACHO 176.18833.411	-0.90	0.26	6600			2.00			0.51
Z Mic	-1.51	0.45	6098	5950	6246	1.86	0.60	2.03	0.52
AW Mic	-2.16	0.39	7522			3.05			0.69
RV Oct	-1.64	0.46	6247	6050	6443	1.84	1.70	1.94	0.51
UV Oct	-1.75	0.35	6243	6050	6435	1.88	1.70	2.00	0.52
V 413 Oph	-0.75	0.30	7120			2.37			0.52
V 445 Oph	0.11	-0.05	6647	6450	6818	2.62	2.43	2.94	0.52
AO Peg	-1.26	0.39	6342			2.55			0.60
AV Peg	-0.19	-0.11	6607	6513	6700	2.61	2.48	2.70	0.52
BH Peg	-1.17	0.40	6500			2.50			0.55
DH Peg	-1.31	0.44	7002	6500	7278	2.73	2.50	2.95	0.59
AR Per	-0.29	0.02	6422	6315	6500	2.79	2.50	3.00	0.57
RU Psc	-2.04	0.51	6500			2.50			0.60
HH Pup	-0.93	-0.08	6250			2.00			0.52
V 701 Pup	-2.90	0.48	7200			2.50			0.57
VW Scl	-1.22	0.35	6850			2.30			0.52
SDSS J170733.93+585059.7	-2.79	0.89	6475	6250	6700	3.68	2.38	4.20	-
VY Ser	-1.78	0.35	6075	5900	6400	2.32	1.85	2.75	0.59
AN Ser	0.00	-0.20	6575	6500	6650	2.45	2.30	2.60	0.51
V 456 Ser	-2.64	0.32	6600			2.45			0.60
T Sex	-1.55	0.26	7225			2.95			0.63
V 440 Sgr	-1.16	0.36	6874	6269	7400	2.62	2.15	2.93	0.55
V 1645 Sgr	-1.94	0.39	6200			2.00			0.54
W Tuc	-1.76	0.32	6100			1.82			0.53
BK Tuc	-1.65	0.38	6220			2.07			0.53
TYC 4887-622-1	-1.79	0.31	7100			2.10			0.53
TYC 6644-1306-1	-1.78	0.33	7250			2.50			0.56

1	2	3	4	5	6	7	8	9	10
TYC 8776-1214-1	-2.72	0.44	7100			2.17			0.54
RV UMa	-1.25	0.35	6413	6370	6500	2.33	2.27	2.50	0.54
TU UMa	-1.41	0.32	6231	6116	6500	2.44	2.10	2.75	0.58
CD Vel	-1.67	0.38	6208	6050	6366	1.95	1.70	2.10	0.52
ST Vir	-0.85	0.13	6300			2.08			0.52
UU Vir	-0.86	0.30	6269	6225	6333	2.49	1.97	2.83	0.56
UV Vir	-1.10	0.42	7550			2.10			0.51
AS Vir	-1.68	0.41	6232	6000	6436	1.80	1.70	1.87	0.51
DO Vir	-1.57	0.33	6115			1.50			< 0.50